ISBN: 978-3-95450-233-2 ISSN: 2673-5504 doi:10.18429/JACoW-SRF2021-WEPTEV016

FIELD EMISSION STUDIES DURING ESS CRYOMODULE TESTS AT CEA SACLAY

Enrico Cenni, Matthieu Baudrier, Guillaume Devanz, Luc Maurice, Olivier Piquet
CEA Université Paris-Saclay, Gif-sur-Yvette, France

Abstract

For the development of efficient superconducting cavities, field emission is an important parasitic phenomena to monitor. A diagnostic system composed of Geiger-Mueller (G-M) probes, NaI(Tl) scintillators are placed in the cryomodule test stand. Collected data is analysed and confronted to particle tracking simulation and electro magnetic shower code. With such systematic analysis we aim to identify the most probable field emission location and hence help to improve clean procedures during assembly and operation.

INTRODUCTION

In addition to the production of the 30 medium and high beta cryomodules of the European Spallation Source (ESS) LINAC, CEA perform the test at high RF power of two prototype cryomodules and of the three first cryomodules of each type assembled at CEA Saclay. We present the results and analysis concerning the third cryomodule (i.e. CM03) for the medium beta section performance with a particular attention to its field emission behavior. The four cavities installed in the cryomodule were manufactured and prepared by Zanon Research&Innovation under the supervision of INFN LASA. The string assembly were done at CEA Saclay by a subcontractor, while the power test was performed by CEA personnel [1,2]

EXPERIMENTAL SET UP

CEA currently tested two cryomodule prototypes and three from the medium beta section series, which will be re-tested at ESS main site. In this paper we will mainly focus on the last cryomodule, namely CM03.

Cavities and Cryomodule

The cryomodule accommodate four medium beta cavity manufactured with fine grain high purity niobium [3]. In Table 1 are summarized the most significant cavity RF parameters.

Table 1: Design Parameters for Medium Beta Cavities [3]

Design parameters	Value
Geometrical beta - $\leftrightarrows_{geom}/\leftrightarrows_{opt}$	0.67/0.705
Nominal gradient E_{acc} [MV/m]	16.7
Q_0 at nominal gradient	>5x10^9
G [Ω]	198.8
R/Q [Ω]	374
E_{pk}/E_{acc}	2.55
B_{pk}/E_{acc} [mT/(MV/m)]	4.95
E_{pk}@nominal E_{acc} [MV/m]	42.6
B_{pk}@nominal E_{acc} [mT]	83

The two most relevant quantities concerning field emission are the ratio E_{pk}/E_{acc} and the accelerating field required during operation. This is due to the strong dependence of field emission current and surface electric field as demonstrated by Fowler and Nordheim [4] with equation (1).

$$J = \frac{A(\beta E_{surf})^2}{\varphi} e^{-\frac{B\varphi^{1.5}}{\beta E_{surf}}} \quad [\frac{A}{m^2}] \qquad (1)$$

where A and B are constant, φ is the material work function, E_{surf} is the electric field on the surface and $\leftrightarrows$ is the geometrical enhancing factor due to surface asperity.

In Fig. 1 is shown a section of the medium beta cryomodule highlighting the main components and a longitudinal cross section view.

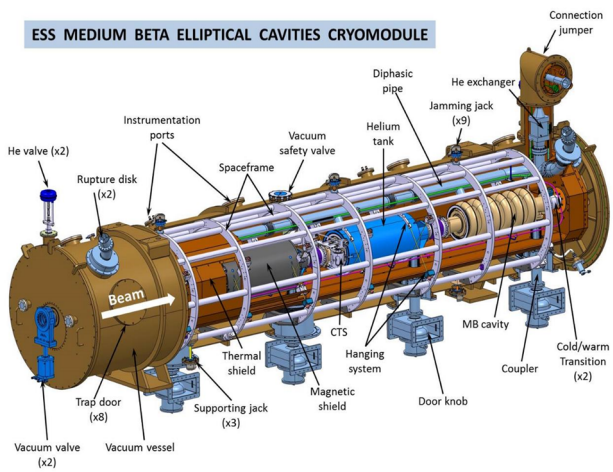

Figure 1: Medium beta cavity cryomodule main components highlight.

Details about cryomodule design parameters are given elsewhere [1,5], here it is worth to recall that the static heat load on the 2K bath is estimated to be around 17W, while the dynamic heat load due to cavity operation is about 20W. Each cavity at nominal field can dissipate about 5W corresponding to a quality factor bigger than 5x10^9 (assuming a machine duty factor around 4%).

Gamma Ray Diagnostic System

A cryomodule test stand has been refurbished at Saclay in order to perform all the required high power test. As part of the new test, set up a gamma ray diagnostic system has been developed and upgrades are foreseen for future tests. A previous set up has been described in a previous publication [6], here will be discussed details concerning the latest cryomodule power test on CM03. In Fig. 2 is shown a medium beta cryomodule installed in the test stand with RF and cryogenic systems connected.

ISBN: 978-3-95450-233-2 ISSN: 2673-5504 doi:10.18429/JACoW-SRF2021-WEPTEV016

Figure 2: Medium beta cryomodule (CMM) installed in the test stand at CEA Saclay.

The current set up consist of two NaI(Tl) scintillators connected to a photo multiplier and a multichannel analyser and six Geiger-Muller counters (G-M), in Fig. 3 are shown their location when cavity #2 is powered.

The power tests are performed mostly one cavity at the time, for each cavity power rise four G-M are placed around the vacuum vessel at the cavity location, while two are always fixed at the cryomodule ends. One of the scintillator is moved in front of the power coupler while the second is fixed at the cryomodule end (jumper side), above the beam pipe gate valve. In this way for each cavity, we can obtain a radial and longitudinal radiation distribution.

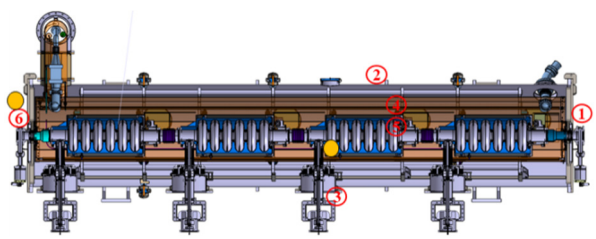

Figure 3: Medium beta cryomodule (CMM), NaI(Tl) scintillators (yellow dots) and a dose rate G-M detectors (numbered red circle) cavity are numbered from right to left (CAV1-CAV4).

Figure 4 presents the scintillator set up: a lead shielding was built around it in order to limit pile up events during operation.

SIMULATION AND DATA ANALYSIS

In this section at first we will present the experimental results obtained during cryomodule power test. The data are collected continuously during the test by means of EPICS interface, but here will be shown only the data where cavities operate at their nominal field and duty cycle. In Fig. 5 is shown a set of data, from EPICS, during cavity #4 power rise and operation at nominal field.

Figure 4: NaI(Tl) scintillator set up during previous cryomodule test, shielding and collimator aperture are shown respectively on the bottom-left and top-right corner of the figure.

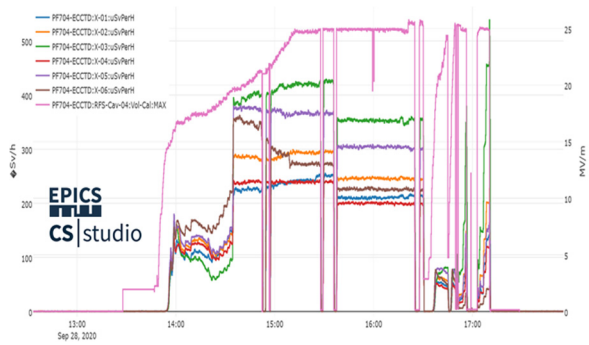

Figure 5: EPCIS data for cavity #4 power rise and operation at nominal field and duty factor, pink line is the accelerating field while others represent Geiger-Muller counter signal (cps).

Finally, data will be analysed by means of particle tracking code and electro magnetic shower Monte Carlo simulation.

Gamma Detectors Data

The Geiger-Muller counters consist of LB6500-4 H10 connected to a LB5340 data logger, their position is sketched in Fig. 6. In Table 2 are presented the recorded dose rate (μSv/h) for each cavity from detectors located at radial position (GM-2,3,4 and 5) with respect to the beam pipe axis.

Table 2: Dose Rate at Nominal Operation (Radial Position)

GM	CAV #1	CAV #2	CAV #3	CAV #4
#		μSv/h		
2	161	352	107	916
3	58	88	75	1615
4	178	338	85	521
5	155	350	100	1297

ISBN: 978-3-95450-233-2 ISSN: 2673-5504 doi:10.18429/JACoW-SRF2021-WEPTEV016

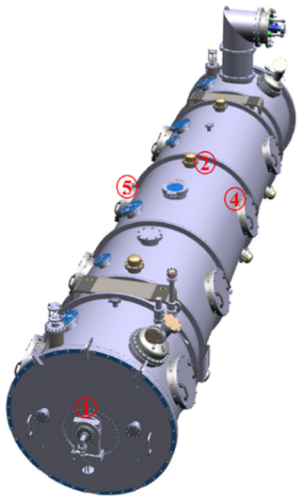

Figure 6: Geiger-Muller position with respect to the cryomodule (top view), this specific configuration is used when cavity #2 is powered up.

In Fig. 7 are presented the integrated dose rate over all the detectors located on radial position (GM2+3+4+5) with respect to the beam line.

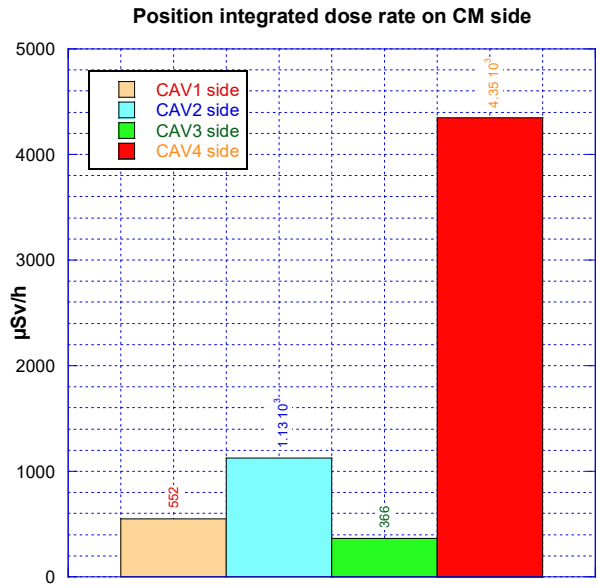

Figure 7: Integrated dose rate over all radial detectors.

Clearly cavity #4 shows a stronger field emission with respect to the other cavities. Its behaviour was also closely related to its cryogenic consumption with respect to the other cavities in the string. Despite some approximation we were able to estimate that the dynamic cryogenic consumption of the first three cavities was about 2W when the cavities operated at nominal field and duty cycle, while cavity #4 was typically around 5W. It represent still an acceptable value, but degraded with respect to the one observed in the vertical cryostat.

In Fig. 8 is shown the radiation distribution (polar plot) with respect to the cryomodule for each cavity operating at nominal field and duty cycle.

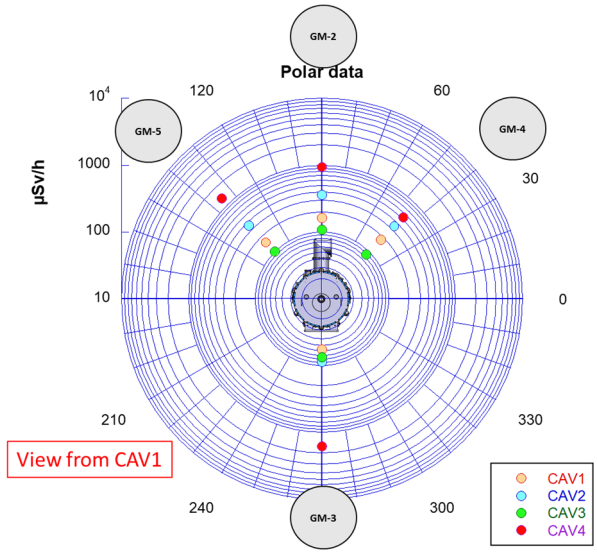

Figure 8: Radiation pattern polar plot around the cryomodule with respect to each cavity operating at nominal accelerating field and duty cycle.

In Fig. 9 is shown an energy spectrum recorded by the multi channel analyser connected to the NaI(Tl) scintillator located on the cryomodule side roughly at the same height of the beam axis close the fundamental power coupler. The end point energy is about 2.5MeV.

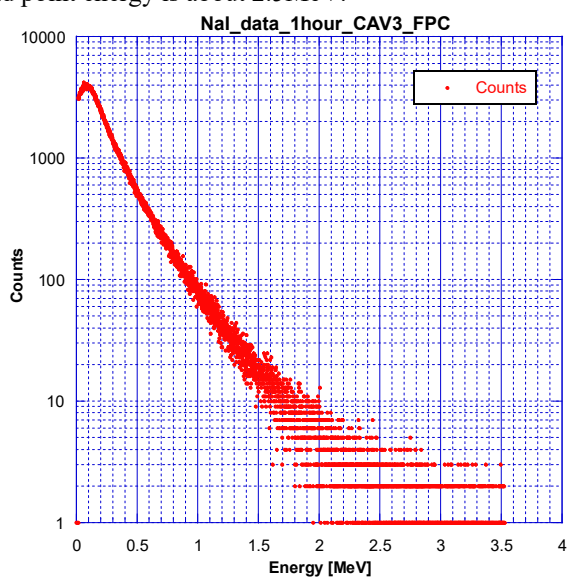

Figure 9: Data collected with the scintillator detector located in front of the fundamental power coupler (FPC) during the cavity power rise, the accelerating field was kept about 16.7 MV/m in the π-mode for one hour.

Particle Tracking Code (Electrons in the Cavity)

The tracking code [7] consist of a Runge-Kutta integration algorithm (4th order) of relativistic particle dynamics, electrons are followed from the emitter (typically on the cavity iris) to the landing point. A set of 50 emitters, 1 mm distant from one another, are placed on each iris. The RF phase is scanned with 1° step. The field map is imported from Superfish code [8].

ISBN: 978-3-95450-233-2 ISSN: 2673-5504 doi:10.18429/JACoW-SRF2021-WEPTEV016

The electron energy at the impact, their impact angle and position are recorded along with the RF phase and the departure point. The data are then post-processed by a set of Gnuplot scripts. In Fig. 10 is shown a simulation result with emitters located on the 5th cavity iris.

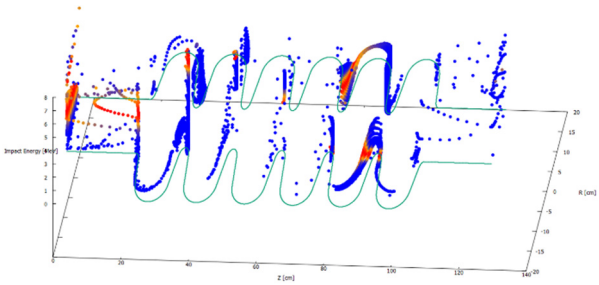

Figure 10: Medium beta cavity particle tracking, emitters are located on the 5th iris (from left), E_{acc}=17MV/m, trajectories are calculated at each 1° phase step. X-Y axis are used for cavity geometry and impact location, Z axis is used for impact energy and colours from green to red are used in proportion with the electron current computed by Eq. (1) (green=low current, red=high current).

In Fig. 11 is shown the electron energy spectrum originating from 5th cavity iris and impacting on the niobium surface. Blue bins represent electron that remain inside the cavity, red bins are for the one escaping from the left beam pipe and green bins for the one escaping from the right beam pipe. The specific spectrum is generated by imposing a 17MV/m accelerating field in the cavity. As a rule of thumb we observed that roughly 80-90% of electron trajectories remain inside the cavity, and their energy spectrum is between 1-2MeV independently from which iris they are originated.

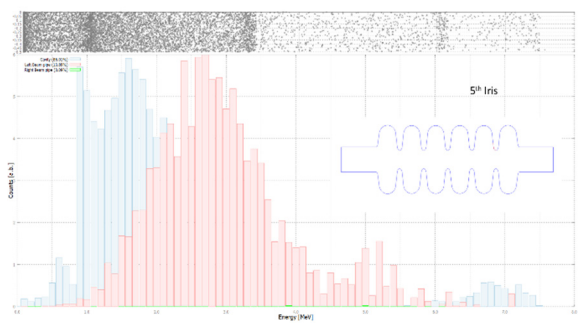

Figure 11: Energy spectra from particle tracking on medium beta cavity with emitters located on 5th iris and accelerating field of 17 MV/m, red and green bins represent trajectories that end on the cavity beam pipes while blue bins represent impact location inside the cavity. Binning is done every 100 keV and the counting is proportional to Eq. (1).

Electromagnetic Shower Monte Carlo Simulation (GEANT4)

A first study iteration has been performed on a cryomodule simplified model by means of a Monte Carlo simulation toolkit (GEANT4) [9]. Despite using the correct material composition and thickness, the geometry is greatly simplified, as shown in Fig. 12, in order to have a first approximate result and radiation pattern general behaviour. We started by looking at which kind of spectrum we could expect on the cryomodule side (radial direction with respect to the beam pipe axis). All the cryomodule subcomponents are modelled as cylindrical shell with the proper thickness and material.

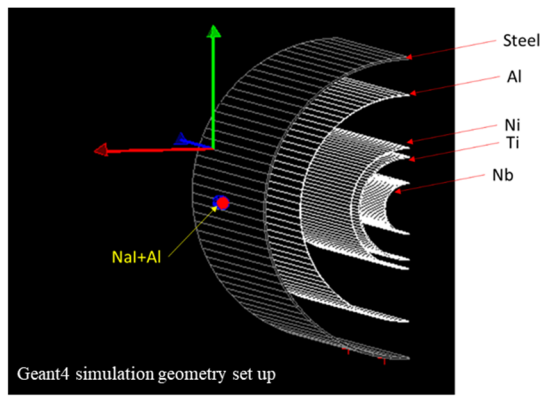

Figure 12: Geant4 cryomodule simplified model, all components are cylindrical cell, from the innermost part Niobium (cavity), Titanium (He tank), Nickel (Magnetic shield), Aluminium (thermal shield) and Steel (vacuum vessel), the detector consist of a NaI crystal with Aluminium casing.

After setting up a proper geometry the field emitted electron beam has been simulated as mono energetic, in Fig. 13 is shown a shower generated by electrons impinging on the Niobium with 2 MeV kinetic energy.

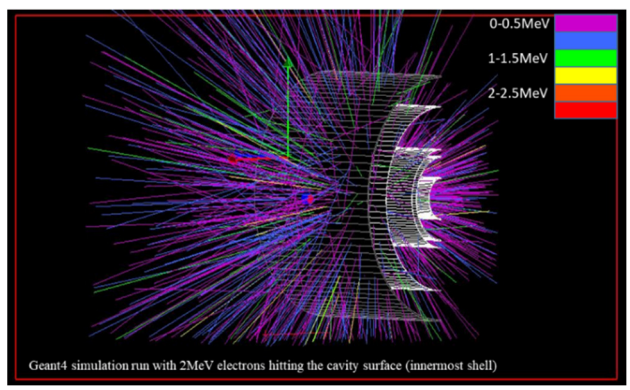

Figure 13: Shower generated by 2MeV electrons impinging on the niobium.

In Fig. 14 is shown the energy spectrum originated by the photon energy deposited in the detector. Each set of points represent different electron impact angles with respect to the detector, where 0° represent electrons heading directly towards the detector. Each simulation run consist of 107 electrons.

This preliminary results show a good agreement with the energy spectra recorded during cryomodule power test

SUMMARY AND OUTLOOK

We have implemented a set of tools in order to detect and analyse radiation produced by field-emitted electrons

ISBN: 978-3-95450-233-2 ISSN: 2673-5504 doi:10.18429/JACoW-SRF2021-WEPTEV016

impacting on cavity surface. A good agreement is observed between simulation and experimental results despite some simplified model has been used. It proves that our systematic approach consisting of detailed radiation mapping around the cryomodule and analysis by means of particle tracking code and Monte Carlo simulation can indeed help to have a better understanding of field emission phenomena during cryomodule tests and operation [10].

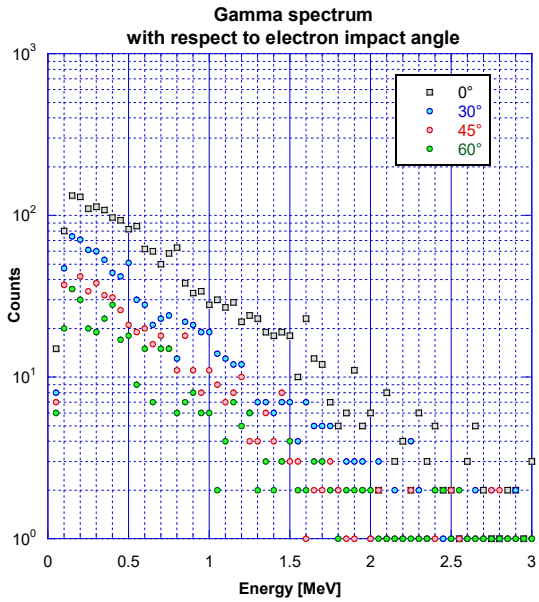

Figure 14: Energy spectrum generated by photons reaching the detector, each set of points represent a different electron impact angle with respect to the detector position.

Furthermore, CEA Saclay is continuously improving the detection capability for both vertical and cryomodule test stand. In the future, more detectors (G-M and scintillators) will be added to gain a more detailed view of the radiation distribution around the cavities and hence a more precise location of field emission sources. More detailed model will be implemented in the GEANT4 simulation in order to capture characteristic features of the radiation pattern generated by field-emitted electrons. In Fig. 15 is shown a significant simulation upgrade, by means of a detailed cryomodule geometry. We plan to develop, on the basis of this geometry, a more realistic simulation taking into account a precise electron beam model by exploiting particle tracking results.

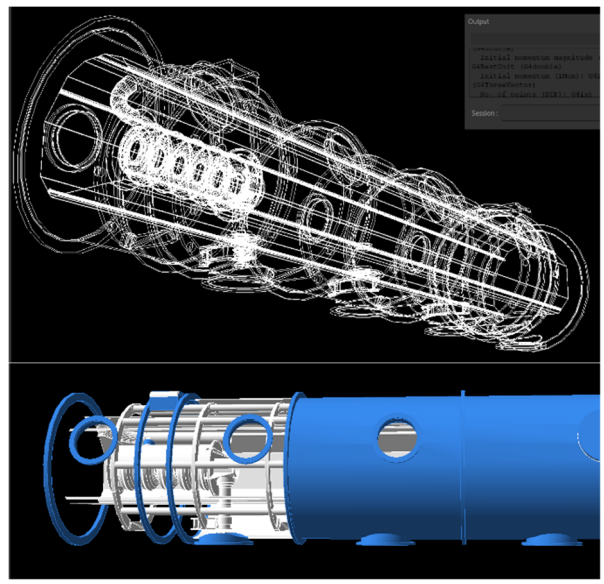

Figure 15: Detailed cryomodule geometry for GEANT4 simulation.

REFERENCES

[1] P. Bosland *et al.*, "Tests at High RF Power of the ESS Medium Beta Cryomodule Demonstrator", in *Proc. IPAC'19*, Melbourne, Australia, May 2019, pp. 1940-1943. doi:10.18429/JACoW-IPAC2019-TUPTS006

[2] C. Madec *et al.*, "The ESS Elliptical Cavity Cryomodules Production at CEA", in *Proc. IPAC'21*, Campinas, Brazil, May 2021, pp. 2536-2539. doi:10.18429/JACoW-IPAC2021-WEXB01

[3] P. Michelato *et al.*, "ESS Medium and High Beta Cavity Prototypes", in *Proc. IPAC'16*, Busan, Korea, May 2016, pp. 2138-2140. doi:10.18429/JACoW-IPAC2016-WEPMB011

[4] R. H. Fowler and L. Nordheim, "Electron Emission in Intense Electric Fields", *Proc. R. Soc. London Ser. A*, vol. 119, p. 173, 1928. doi:10.1098/rspa.1928.0091

[5] G. Devanz *et al.*, "ESS Elliptical Cavities and Cryomodules", in *Proc. SRF'13*, Paris, France, Sep. 2013, paper FRIOC02, pp. 1218-1222.

[6] E. Cenni *et al.*, "Field Emission Studies on ESS Elliptical Prototype Cavities at CEA Saclay", in *Proc. SRF'19*, Dresden, Germany, Jun.-Jul. 2019, pp. 1147-1151. doi:10.18429/JACoW-SRF2019-THP097

[7] G. Wu, fishpact, an experimental code for electron activity studies in SRF cavities. https://code.google.com/archive/p/fishpact/

[8] K. Halbach and R.F. Holsinger, "Superfish a computer program for evaluation of rf cavities with cylindrical symmetry", *Part. Accel.*, vol. 7, pp. 213-222, 1976.

[9] S. Agostinelli *et al.*, "Geant4—a simulation toolkit", *Nucl. Instrum. Methods A*, vol. 506, p. 250, 2003. doi:10.1016/S0168-9002(03)01368-8

[10] H. Sakai *et al.*, "Field emission studies in vertical test and during cryomodule operation using precise x-ray mapping system", *Phys. Rev. Accel. Beams*, vol. 22, p. 022002, 2019. doi:10.1103/PhysRevAccelBeams.22.022002